INTERNATIONAL JOURNAL FOR NUMERICAL METHODS IN ENGINEERING, VOL. 11, 683–708 (1977)

A STRATEGY FOR THE SOLUTION OF PROBLEMS INVOLVING LARGE DEFLECTIONS, PLASTICITY AND CREEP

DAVID BUSHNELL†
Lockheed Palo Alto Research Laboratory, Palo Alto, California, U.S.A.

SUMMARY

A strategy for solving problems involving simultaneously occurring large deflections, elastic-plastic material behaviour, and primary creep is described. The incremental procedure involves a double iteration loop at each load level or time. In the inner loop the material properties are held constant and the non-linear equilibrium equations are solved by the Newton–Raphson method. These equations are formulated in terms of the tangent stiffness. In the outer loop the plastic and creep strains are determined and the tangent stiffness properties are updated with use of a subincremental algorithm. The magnitude of each time subincrement is determined such that the change in effective stress is less than a preset percentage of the effective stress. The strategy is implemented in a computer pogram, BOSOR 5, for the analysis of shells of revolution. Examples are given of elastic-plastic deformations of a centrally loaded flat plate and elastic-plastic-creep deformations of a beam in bending. The major benefits of the subincremental technique are the increased reliability with which problems involving non-linear plastic and time-dependent material behaviour can be solved and the greatly relaxed requirement on the number of load or time increments needed for satisfactory results.

INTRODUCTION

The high speed digital computer has enabled analysts to construct elaborate models of structures, including large deflection effects and material non-linearity. There are several recent excellent surveys of the various approaches: Tillerson *et al.*[1] review numerical methods used to solve non-linear equations; Armen[2] describes several analytical models of multi-axial plasticity; Nickell[3] gives a survey of techniques for treatment of creep and reviews many widely used computer programs in which creep is included; Hunsaker *et al.*[4] present comparisons between test and theory for currently used models of elastic-plastic material behaviour. Therefore a review of methods will not be included here.

The purpose of this paper is to explain in detail a 'subincremental' numerical strategy for the solution of problems in which large deflections, plasticity and primary creep are simultaneously present. This strategy is an extension of a procedure described in Reference 5. It includes modifications for the solution of problems involving primary creep without the occurrence of numerical instability. The method has been incorporated into the BOSOR 5 computer program for analysis of shells of revolution[6], and it can be used for more general configurations. Huffington[7] was the first to point out the advantage of using a subincremental method. Nayak and Zienkiewicz[8] and Stricklin *et al.*[9] have incorporated versions of it into their computer programs.

† Staff Scientist.

Received 13 June 1975
Revised 24 February 1976

The subincremental method

Before a detailed description of the analysis is presented a brief explanation will be given of what the 'subincremental' technique is and why it is needed.

In practically all non-linear analyses the load is applied incrementally and the response is determined for each value of the load. Each load level involves the solution of a system of simultaneous algebraic equations, the rank of this sytem being equal to the number of degrees-of-freedom in the discretized mathematical model. Let us henceforth refer to this system of simultaneous equations as 'System A'. In most analyses in which material non-linearity is included, the iteration loop for the solution of System A contains calculations for determination of the plastic strain components. Usually these quantities are obtained in a one-step process in which the total increments of strain accumulated from one load level to the next are allocated among elastic, plastic, and possibly creep components. The relative magnitudes of the various components are known, at least as the load step begins, because the analysis contains a flow theory and the position of each material point in stress space is known from the converged results associated with the previous load level. The direction of plastic flow for each material point is generally considered to be constant for the entire load increment. For example, it may be assumed that this direction is parallel to the normal to the yield surface at a location in stress space determined by the converged result at the previous load level. Determination of the plastic strain components requires in the general three-dimensional case solution of a set of six simultaneous equations at each material point and in the case of axisymmetric deformations of thin shells the solution of two simultaneous equations at each material point. We shall henceforth refer to this small system of simultaneous equations as 'System B'.

The analysis presented here differs from most other analyses in two respects. The calculation of the plastic and creep strain components is removed from the iteration loop in which System A is solved, and a subincremental approach is used for calculation of the plastic and creep strain components so that the direction of flow is permitted to change continuously within a single load interval.

The removal of the calculations involving plastic flow from the iteration loop for the solution of System A removes an objection pointed out by Tillerson *et al.*[1] to the use of the Newton–Raphson method for problems involving elastic-plastic material. They found that the 'Newton–Raphson' procedure failed to converge if they used the tangent stiffness approach because of indications of alternative loading and unloading from iteration to iteration. Since the coefficients of their System A changed in a discontinuous manner in successive iterations, their strategy could not really be called a Newton method. In the present analysis the Newton–Raphson method is used with success.

In the subincremental process the total increments of strain accumulated from one load level to the next are divided into subincrements of a certain magnitude. For each subincrement the direction of plastic flow is considered to be constant, given by the normal to the yield surface at a location in stress space determined by the result at a previous subincrement. For each strain subincrement the stress subincrements are determined from the flow law and the given relationship between effective stress subincrement and effective plastic strain subincrement (the uniaxial stress–strain curve). Thus, the equation System B is solved for each subincrement and each material point.

The need for the subincremental method

Why is the subincremental method needed? This question can perhaps be best answered with reference to the equations which form the simultaneous System B (creep neglected):

$$\{\Delta\varepsilon\} = [D^{-1}]\{\Delta\sigma\} + \Delta\bar{\varepsilon}^{p}\left\{\frac{\partial\bar{\sigma}}{\partial\sigma}\right\}_0 \tag{1a}$$

$$= [D^{-1}]\{\Delta\sigma\} + \frac{E - E_T}{EE_T}\Delta\bar{\sigma}\left\{\frac{\partial\bar{\sigma}}{\partial\sigma}\right\}_0 \tag{1b}$$

$$= [D^{-1}]\{\Delta\sigma\} + \frac{E - E_T}{EE_T}f(\Delta\sigma_{ij})\left\{\frac{\partial\bar{\sigma}}{\partial\sigma}\right\}_0 \tag{1c}$$

In equations (1a)–(1c) the left-hand side $\{\Delta\varepsilon\}$ is the known vector of strain component increments; $\{\Delta\sigma\}$ is the unknown vector of stress component increments; $\Delta\bar{\varepsilon}^{p}$ is the unknown effective plastic strain increment, which in Eq. (1b) is expressed in terms of the effective stress increment $\Delta\bar{\sigma}$ and in Eq. (1c) in terms of the effective stress component increments through the non-linear function $f(\Delta\sigma_{ij})$. The vector $\{\partial\bar{\sigma}/\partial\sigma\}_0$ represents the components of a unit normal to the yield surface at a point in stress space fixed by the stress components $\{\sigma_0\}$ calculated at the previous load level at which a converged solution has been obtained. The non-linear System B can in principle be solved for the stress component increments $\{\Delta\sigma\}$. However, it often happens, especially at stress concentrations where $\{\Delta\varepsilon\}$ is relatively large, that System B does not have a solution. Figure 1 demonstrates what happens. A sequence of values of $\Delta\bar{\varepsilon}^{p}$ can be tried in Eq. (1a) to generate the solid curve in Figure (1a). The dashed curve is the stress–strain curve. Ideally, the value of $\Delta\bar{\varepsilon}^{p}$ which satisfies all of the conditions is computed as one of the intersections of the two curves. Indeed, solutions can be obtained in this manner as long as the effective strain increment is less than about 0·1 per cent. For larger strain increments, however, the result shown in Figure 1(b) is common. The 'subincrement' method prevents this anomaly.

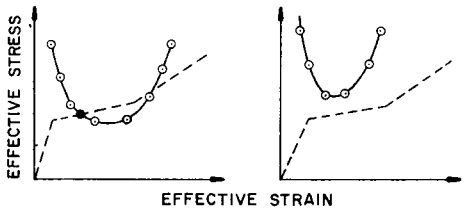

Figure 1. Schematic representation of the solution of equations (1) without use of the subincremental method

Another problem in calculating $\{\Delta\sigma\}$ from Eqs. (1) arises from the fact that the tangent modulus E_T is a non-linear function of $\bar{\varepsilon}^{p}$ or $\bar{\sigma}$. In the analysis to be described later, the actual stress–strain curve is replaced by a series of straight line segments. As the load is increased from one level to the next, E_T changes in a discontinuous way that is not possible to express in a simple functional form. It is necessary to divide the increment such that at every material point E_T is constant within any subincrement.

Paths in strain space and stress space

The subincremental method is especially advantageous when applied to problems in which the paths followed by material points have less curvature in strain space than in stress space, which is usually the case for thin shells stressed beyond the proportional limit. Figures 2 and 3 illustrate this behaviour. Figure 2 shows the paths in strain and stress space followed by the point for which the effective strain is maximum in an internally pressurized mild steel torispherical

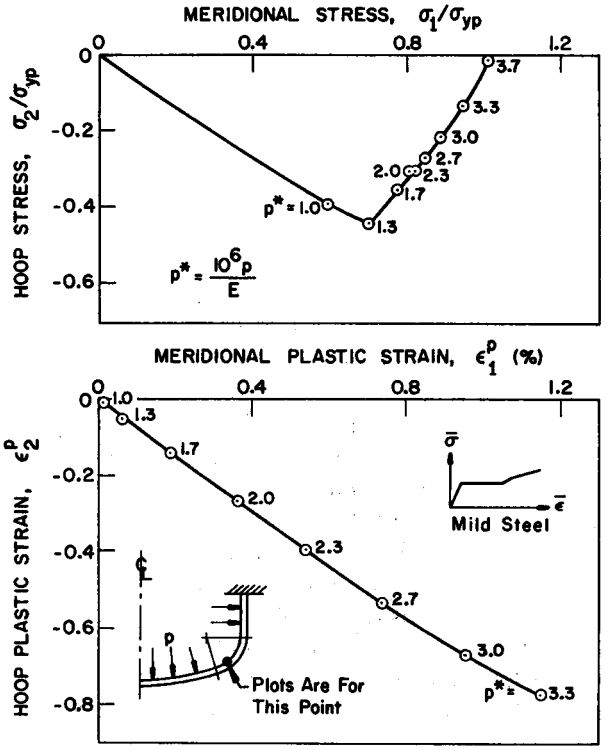

Figure 2. Paths followed in stress space and strain space by a material point in an internally pressurized torispherical vessel head of mild steel

pressure vessel head. Whereas the straining of the material is nearly proportional throughout the range of pressure, the loading of the material is approximately proportional only until the effective stress reaches the yield stress, after which the path in stress space follows the yield surface in a counterclock-wise direction. A similar phenomenon occurs for a centrally loaded flat plate, results for which are shown in Figure 3. Here the path is strain space is more curved because of the direction of loading and certain pecularities of the geometrically non-linear behaviour. Still the curvature of this path is not as great as that of the path in stress space. The subincremental method is especially suitable for problems such as these because of the non-proportional loading of the material. If the subincremental method had not been used, many more load steps would have been required to avoid the aforementioned difficulties associated with the solution of Eqs. (1).

Fewer load steps needed

A basic advantage of the subincremental method, then, is that it allows the use of much larger load increments than would otherwise be possible. The magnitude of the subincrement can be fixed such that in Eqs. (1a)–(1c) E_T is constant within a subincrement and the non-linear function $f(\Delta\sigma_{ij})$, now $f(\mathrm{d}\sigma_{ij})$, where 'd' indicates 'subincrement', can be linearized. Furthermore, if the material creeps the magnitude of each subincrement can be established such that the change in effective stress during a subincrement is less than a certain preset percentage of the current effective stress. This criterion is important because the creep law used here is derived from tests in which the stress is held constant.

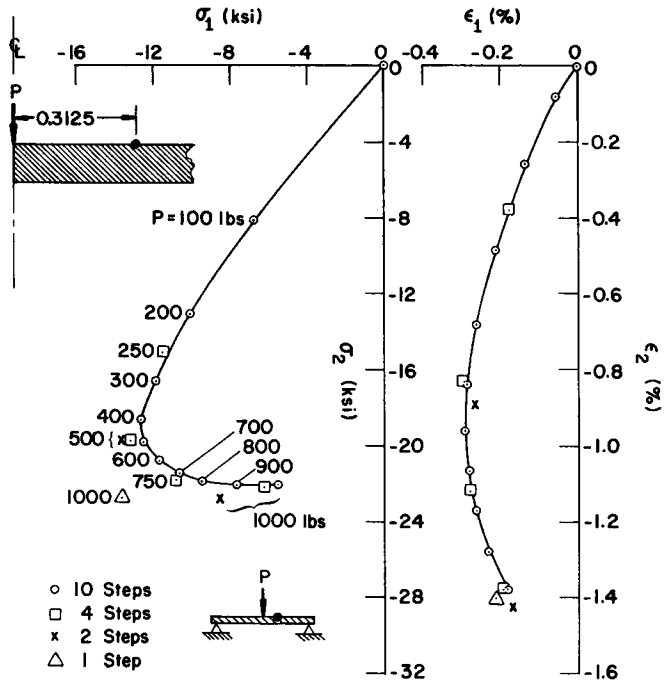

Figure 3. Paths followed in stress space and strain space by a material point in a circular flat plate with a concentrated load, P

Trade-off in computer time

There is a trade-off in the use of the subincremental method. Fewer load steps need to be taken to cover a given load range, which generally means that the often large simultaneous equation System A must be solved fewer times than would otherwise be the case. On the other hand, incremental stress components and plastic and creep strain components must be calculated for each subincrement. Therefore, relatively more computer time must be used for determination of the behaviour of the material. A great advantage of the subincremental method is that it makes the elastic-plastic analysis more reliable. The maximum size of a subincrement is preset. Therefore, more subincrements will automatically be used for material points corresponding to stress concentrations. In this way the errors incurred by linearization of Eqs. (1a)–(1c) and by changes in the direction of plastic flow within an increment are made less severe.

Creep

Nickell[3] gives a survey of computer programs in which primary and secondary creep are accounted for. Basically there are two approaches to the creep problem, the 'equation-of-state' approach and the 'hereditary' approach. In the former model the effective creep strain rate $\dot{\bar{\varepsilon}}^c$ derived for conditions of changing stress is considered to be of either of the forms

$$\dot{\bar{\varepsilon}}^c = f(\bar{\sigma}, T, t) \quad \text{or} \quad \dot{\bar{\varepsilon}}^c = g(\bar{\sigma}, T, \bar{\varepsilon}^c) \tag{2}$$

in which the first is known as the 'time hardening' model and the second is known as the 'strain hardening' model. Greenstreet *et al.*[10] present modifications to the strain hardening model in

order to eliminate certain numerical anomalies that occur under reversed loading. In the hereditary approach, initially formulated by Rabotnov[11] and favoured by Rashid[12], the effective creep strain is expressed as a convolution integral over time.

Tests on specimens subjected to a program of stepped uniaxial loads indicate that the strain hardening model should be used. In particular, Russel and Kobayashi[13] found that for 6AL4V titanium specimens between 1,000° and 1,200° the strain hardening model was in better agreement with the test results than either the time hardening model, which led to under-estimation of the creep strain, or the hereditary model, which led to over-estimation. Figure 4 shows schematically how the creep strain is computed with use of the strain hardening model.

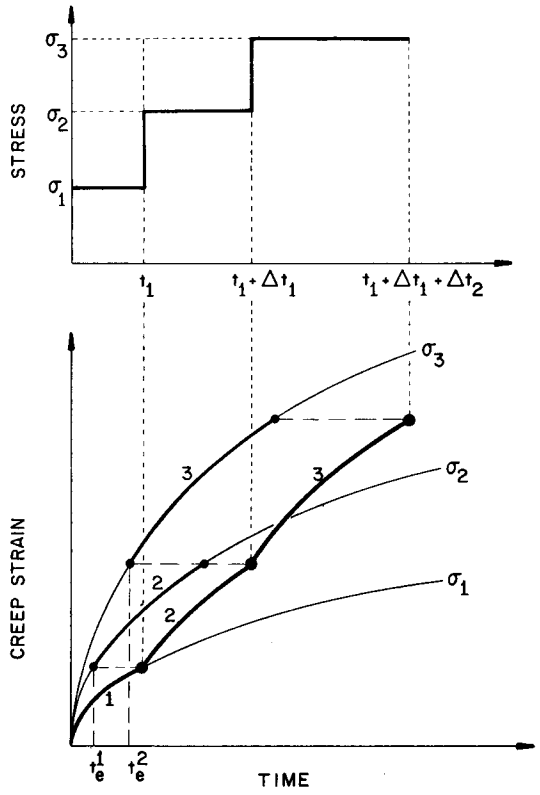

Figure 4. Accumulated creep strain predicted with use of the strain hardening model

The creep strain components in multi-axial applications are determined from a flow rule usually associated with a yield locus. Most computer programs handle creep strains as initial strains rather than modify the stiffness matrix as is done more often for plastic flow. The NEPSAP program written by Sharifi[14] is an exception. Also, most of the codes have some sort of automatic control of the time increment based on change in effective stress or effective creep strain per elastic strain. None of these codes, with the possible exception of that derived by Zienkiewicz *et al.*[15] includes creep in connection with a subincremental method. The analysis of Reference 15 is based on steady creep.

In the present analysis creep is handled in the following way:

1. The equation of state is a power law of the form

$$\bar{\sigma}^{c} = A\bar{\sigma}^{m} t_e^{n} \tag{3}$$

in which t_e is an effective time determined as described later. Crussard[16], in a study of many different materials, found that Eq. (3) could generally be used to fit the experimental data for specimens subjected to constant stress.

2. The method is, for all practical purposes, based on a strain-hardening model, although an element of the time-hardening model creeps into the picture, as shall be seen later.

3. The flow rule is the same as that used for the plastic strains associated with the J_2 invariant. The creep strains cause no change in volume.

4. The creep strains are handled as initial strains, the stiffness matrix being unaffected by them.

ANALYSIS

Basic equations

The BOSOR 5 prebuckling analysis[6] is based on the principle of virtual work, which can be written

$$\delta U = \int_{\text{Volume}} \lfloor \varepsilon - \varepsilon^{p} - \varepsilon^{c} - \varepsilon^{T} \rfloor [D] \{\delta\varepsilon\} \, dV = \delta W \tag{4}$$

where U represents the shell strain energy, and W the work done by external forces. If Eq. (4) is applied to axisymmetric deformations of shells of revolution,

$\lfloor \varepsilon \rfloor$ or $\{\varepsilon\}$ represents the total meridional and circumferential strain components $\lfloor \varepsilon_1, \varepsilon_2 \rfloor$ or $\begin{Bmatrix} \varepsilon_1 \\ \varepsilon_2 \end{Bmatrix}$

$\lfloor \varepsilon^{p} \rfloor$ represents the total plastic strain components $\lfloor \varepsilon_1^{p}, \varepsilon_2^{p} \rfloor$

$\lfloor \varepsilon^{c} \rfloor$ represents the total creep strain components $\lfloor \varepsilon_1^{c}, \varepsilon_2^{c} \rfloor$

$\lfloor \varepsilon^{T} \rfloor$ represents the thermal strain components $\lfloor \varepsilon_1^{T}, \varepsilon_2^{T} \rfloor$

$$[D] \equiv \frac{E}{1-\nu^2} \begin{bmatrix} 1 & \nu \\ \nu & 1 \end{bmatrix}$$

Integration is performed through the shell thickness, around the circumference, and along the meridian. The variation is taken with respect to the dependent variables q_i, $i = 1, 2, \ldots, N$, where q_i is a nodel degree-of-freedom or a Lagrange multiplier and N is the total number of degrees-of-freedom. If

$$\Psi_i \equiv \int_V \lfloor \varepsilon - \varepsilon^{p} - \varepsilon^{c} - \varepsilon^{T} \rfloor [D] \left\{ \frac{\partial \varepsilon}{\partial q_i} \right\} dV - \frac{\partial W}{\partial q_i} \quad (i = 1, 2, \ldots, N) \tag{5}$$

then the principle of virtual work states that for equilibrium,

$$\Psi_i(q_j) = 0 \qquad i = 1, 2, \ldots, N \quad j = 1, 2, \ldots, N \tag{6}$$

Equations (6) are non-linear algebraic equations to be solved by the Newton–Raphson method. For each Newton–Raphson iteration

$$\sum_{j=1}^{N} \frac{\partial \Psi_i}{\partial q_j} \Delta q_j = -\Psi_i \quad i = 1, 2, \ldots, N \tag{7}$$

must be solved for the correction terms Δq. Iterations proceed until $\Delta q_j / q_j < e$, where e is an error control parameter ($e = 0{\cdot}001$ in BOSOR 5). The quantity $\partial \Psi_i / \partial q_j$ is the (i, j)th coefficient of an $N \times N$ matrix of known coefficients which change with each iteration. The coefficient $\partial \Psi_i / \partial q_j$ in Eq. (7) can be calculated from Eq. (5):

$$\frac{\partial \Psi_i}{\partial q_j} = \int_V \left[\lfloor \varepsilon - \varepsilon^{\mathrm{p}} - \varepsilon^{\mathrm{c}} - \varepsilon^{\mathrm{T}} \rfloor [D] \left\{ \frac{\partial^2 \varepsilon}{\partial q_i \, \partial q_j} \right\} + \frac{\partial}{\partial q_j} \left(\lfloor \varepsilon - \varepsilon^{\mathrm{p}} - \varepsilon^{\mathrm{c}} - \varepsilon^{\mathrm{T}} \rfloor [D] \right) \left\{ \frac{\partial \varepsilon}{\partial q_i} \right\} \right] \mathrm{d}V - \frac{\partial^2 W}{\partial q_i \, \partial q_j} \tag{8}$$

Strategy for handling the material non-linearity

In Eq. (8) the creep strain ε^{c} and the thermal strain ε^{T} are assumed to be independent of the nodal point displacements q_j. Two methods for solving incremental plasticity problems are:

(a) the 'initial strain' method

(b) the 'tangent modulus' method

In the 'initial strain' method the plastic strains are treated as 'effective thermal strains'. In Eq. (8) the term ε^{p} is assumed to be independent of the nodal point displacements q_j. Thus, Eq. (8) becomes

$$\frac{\partial \Psi_i}{\partial q_j} = \int_V \left(\lfloor \varepsilon - \varepsilon^{\mathrm{p}} - \varepsilon^{\mathrm{c}} - \varepsilon^{\mathrm{T}} \rfloor [D] \left\{ \frac{\partial^2 \varepsilon}{\partial q_i \, \partial q_j} \right\} + \left\lfloor \frac{\partial \varepsilon}{\partial q_j} \right\rfloor [D] \left\{ \frac{\partial \varepsilon}{\partial q_i} \right\} \right) \mathrm{d}V - \frac{\partial^2 W}{\partial q_i \, \partial q_j} \tag{9}$$

where all quantities are known and independent of q_i and q_j except ε and W.

In the 'tangent stiffness' method, which is used in BOSOR 5, the rates of change of the plastic strain components are expressed in terms of the rates of change of the total strain components.

$$\{\mathrm{d}\varepsilon^{\mathrm{p}}\} = [C]\{\mathrm{d}\varepsilon - \mathrm{d}\varepsilon^{\mathrm{c}} - \mathrm{d}\varepsilon^{\mathrm{T}}\} \tag{10}$$

or, if $[C]$, ε^{c} and ε^{T} are regarded as independent of q_j

$$\frac{\partial \varepsilon^{\mathrm{p}}}{\partial q_j} = [C] \frac{\partial}{\partial q_j} \{\mathrm{d}\varepsilon - \mathrm{d}\varepsilon^{\mathrm{c}} - \mathrm{d}\varepsilon^{\mathrm{T}}\} = [C] \left\{ \frac{\partial \varepsilon}{\partial q_j} \right\} \tag{11}$$

The 2×2 matrix $[C]$ is derived in a following section. If one inserts the right-hand side of Eq. (11) into Eq. (8), one obtains (recalling that $[D]$ is independent of q_j)

$$\left\{ \frac{\partial \Psi_i}{\partial q_j} \right\} = \int_V \left(\lfloor \varepsilon - \varepsilon^{\mathrm{p}} - \varepsilon^{\mathrm{c}} - \varepsilon^{\mathrm{T}} \rfloor [D] \left\{ \frac{\partial^2 \varepsilon}{\partial q_i \, \partial q_j} \right\} + \left\lfloor \frac{\partial \varepsilon}{\partial q_j} \right\rfloor \underbrace{[I - C]^{\mathrm{T}} [D]}_{\substack{\text{'tangent stiffness'} \\ \text{matrix}}} \left\{ \frac{\partial \varepsilon}{\partial q_i} \right\} \right) \mathrm{d}V - \frac{\partial^2 W}{\partial q_i \, \partial q_j} \tag{12}$$

The two element vector ε^{p} which appears in the first term on the right-hand side of Eqs. (5) and (12) is given by

$$\{\varepsilon^{\mathrm{p}}\} = \{\varepsilon_0^{\mathrm{p}} + \Delta\varepsilon^{\mathrm{p}}\} = \{\varepsilon_0^{\mathrm{p}} + [C](\varepsilon - \varepsilon_0)\} \tag{13}$$

in which the subscript $(\ )_0$ denotes 'value obtained when the material properties were last updated'. With use of Eq. (13), one can write Eq. (12) in the form

$$\frac{\partial \Psi_i}{\partial q_j} = \int_V \left(\lfloor \varepsilon \rfloor [D_T] \left\{ \frac{\partial^2 \varepsilon}{\partial q_i \, \partial q_j} \right\} + \left\lfloor \frac{\partial \varepsilon}{\partial q_j} \right\rfloor [D_T] \left\{ \frac{\partial \varepsilon}{\partial q_i} \right\} + \lfloor [C]\varepsilon_0 - \varepsilon_0^p - \varepsilon^c - \varepsilon^T \rfloor [D] \left\{ \frac{\partial^2 \varepsilon}{\partial q_i \, \partial q_j} \right\} \right) dV - \frac{\partial^2 W}{\partial q_i \, \partial q_j} \tag{14}$$

where $[D^T]$ is the tangent stiffness matrix,

$$[D^T] \equiv [I - C]^T [D] \tag{15}$$

The governing equations of the 'tangent stiffness' method for each Newton–Raphson iteration are obtained by insertion of Eqs. (5) and (14) into Eq. (7).

In Eq. (11) the rates of change of the plastic strain components are related to the total strain components by means of the 2×2 matrix $[C]$. The derivation of this 2×2 matrix follows [Eqs. (16)–(24)].

The stress components are given by

$$\{\sigma\} = [D]\{\varepsilon - \varepsilon^p - \varepsilon^c - \varepsilon^T\} \tag{16}$$

and the stress increments by

$$\{\Delta\sigma\} = [D]\{\Delta\varepsilon - \Delta\varepsilon^p - \Delta\varepsilon^c - \Delta\varepsilon^T\} \tag{17}$$

From the condition that the resultant plastic strain increment vector must be normal to the Von Mises yield surface, the following relationships arise:

$$\{\Delta\varepsilon_i^p\} = \left\{ \frac{\partial \bar{\sigma}}{\partial \sigma_i} \right\} \Delta\bar{\varepsilon}^p = \begin{Bmatrix} (\sigma_1 - 1/2\sigma_2)/\bar{\sigma} \\ (\sigma_2 - 1/2\sigma_1)/\bar{\sigma} \end{Bmatrix} \Delta\bar{\varepsilon}^p \qquad (i = 1, 2) \tag{18}$$

where $\Delta\varepsilon_i^p$, $i = 1, 2$ are the incremental plastic strain components; $\Delta\bar{\varepsilon}^p$ is the effective plastic strain increment; σ_i, $i = 1, 2$ are given by Eq. (16); and $\bar{\sigma}$ is the effective stress,

$$\bar{\sigma} = (\sigma_1^2 + \sigma_2^2 - \sigma_1\sigma_2)^{1/2} \tag{19}$$

Premultiplying both sides of Eq. (17) by the row $\lfloor \partial\bar{\sigma}/\partial\sigma \rfloor$ and substituting the right-hand side of Eq. (18) for $\{\Delta\varepsilon^p\}$, one obtains

$$\left\lfloor \frac{\partial \bar{\sigma}}{\partial \sigma} \right\rfloor \{\Delta\varepsilon\} = \overline{\Delta\sigma} = H'\Delta\bar{\varepsilon}^p = \left\lfloor \frac{\partial \bar{\sigma}}{\partial \sigma} \right\rfloor [D] \left(\{\Delta\varepsilon\} - \left\{ \frac{\partial \bar{\sigma}}{\partial \sigma} \right\} \Delta\bar{\varepsilon}^p - \{\Delta\varepsilon^c\} - \{\Delta\varepsilon^T\} \right) \tag{20}$$

Eq. (20) can be solved for $\Delta\bar{\varepsilon}^p$:

$$\Delta\bar{\varepsilon}^p = \frac{\left\lfloor \frac{\partial \bar{\sigma}}{\partial \sigma} \right\rfloor [D](\{\Delta\varepsilon\} - \{\Delta\varepsilon^c\} - \{\Delta\varepsilon^T\})}{H' + \left\lfloor \frac{\partial \bar{\sigma}}{\partial \sigma} \right\rfloor [D] \left\{ \frac{\partial \bar{\sigma}}{\partial \sigma} \right\}} \tag{21}$$

The two elements of the row or column $\{\partial\bar{\sigma}/\partial\sigma\}$ are given in Eq. (18). H' is the slope of the effective stress *vs* effective plastic strain curve, which locally is given by

$$H' = EE_T/(E - E_T) \tag{22}$$

where E_T is the tangent modulus. From Eq. (18) comes the final expression

$$\{\Delta\varepsilon^P\} = [C]\{\Delta\varepsilon - \Delta\varepsilon^c - \Delta\varepsilon^T\} \tag{23}$$

where

$$[C]_{2\times 2} = \frac{\left\{\frac{\partial\bar{\sigma}}{\partial\sigma}\right\}\left\lfloor\frac{\partial\bar{\sigma}}{\partial\sigma}\right\rfloor[D]}{H' + \left\lfloor\frac{\partial\bar{\sigma}}{\partial\sigma}\right\rfloor[D]\left\{\frac{\partial\bar{\sigma}}{\partial\sigma}\right\}} \tag{24}$$

The above formulation follows Stricklin *et al.*[9] Marcal[17] employs a similar procedure.

Solution strategy—a double-iteration loop

The prebuckling iteration strategy is as follows. At each load level or time step there are two nested iteration loops. In the inner loop the set of simultaneous non-linear algebraic equations (7) with given fixed material properties and plastic and creep strains is solved. This is the 'Newton–Raphson loop'. In the outer loop the strain-dependent material properties, the matrix $[C]$, the plastic strain components ε_1^p, ε_2^p, and the creep strain components ε_1^c, ε_2^c are calculated. Double iterations at a given load level continue until the displacements no longer change. In this way the favourable convergence property of the Newton–Raphson procedure is preserved, equilibrium is satisfied within the degree of approximation inherent in a discrete model, and the flow law of the material is satisfied at every point in the structure. This strategy is illustrated in the flow chart shown in Figure 5.

COMPUTATIONAL PROCEDURE FOR OBTAINING PLASTIC AND CREEP STRAINS

A subincremental method for the solution of problems involving large deflections, plasticity, and creep is used in BOSOR 5. As described in the Introduction, this method permits the use of large 'major' load or time increments. (A 'major' increment is one for which the governing equations, called 'System A' in the Introduction, are repeatedly solved by the Newton–Raphson method until convergence is achieved.) If creep is neglected, the 'major' time increment, call it Δt, is subdivided into equal subincrements, dt, such that each effective strain subincrement, $d\bar{\varepsilon}$, is less than 0·0002. It is assumed that the total effective strain increment $\Delta\bar{\varepsilon}$ is subdivided into $\Delta\varepsilon/0{\cdot}0002$ equal subincrements, $d\bar{\varepsilon}$. This strategy is also suitable for some cases in which secondary creep occurs. However, the strategy does not work well for primary creep or for cases in which the creep law has a high power on stress. For example, it is not possible to determine the creep-buckling pressure of a titanium shell with a moderate amount of computer time since the 'major' increments have to be excessively small for early times. The strategy fails for early times because there is a relatively large amount of creep which for reasonable time subincrements leads to prediction of substantial changes in stress. Unless extremely small time increments are used, the change in state of the material as a function of time cannot be predicted with requisite accuracy.

If primary creep is present, the strategy which has been implemented in the BOSOR 5 computer program involves determination of the ith subincrement $dt^{(i)}$ such that the maximum change in effective stress $d\bar{\sigma}_{(i)}$ during each $dt^{(i)}$ is less than a certain fixed percentage of the

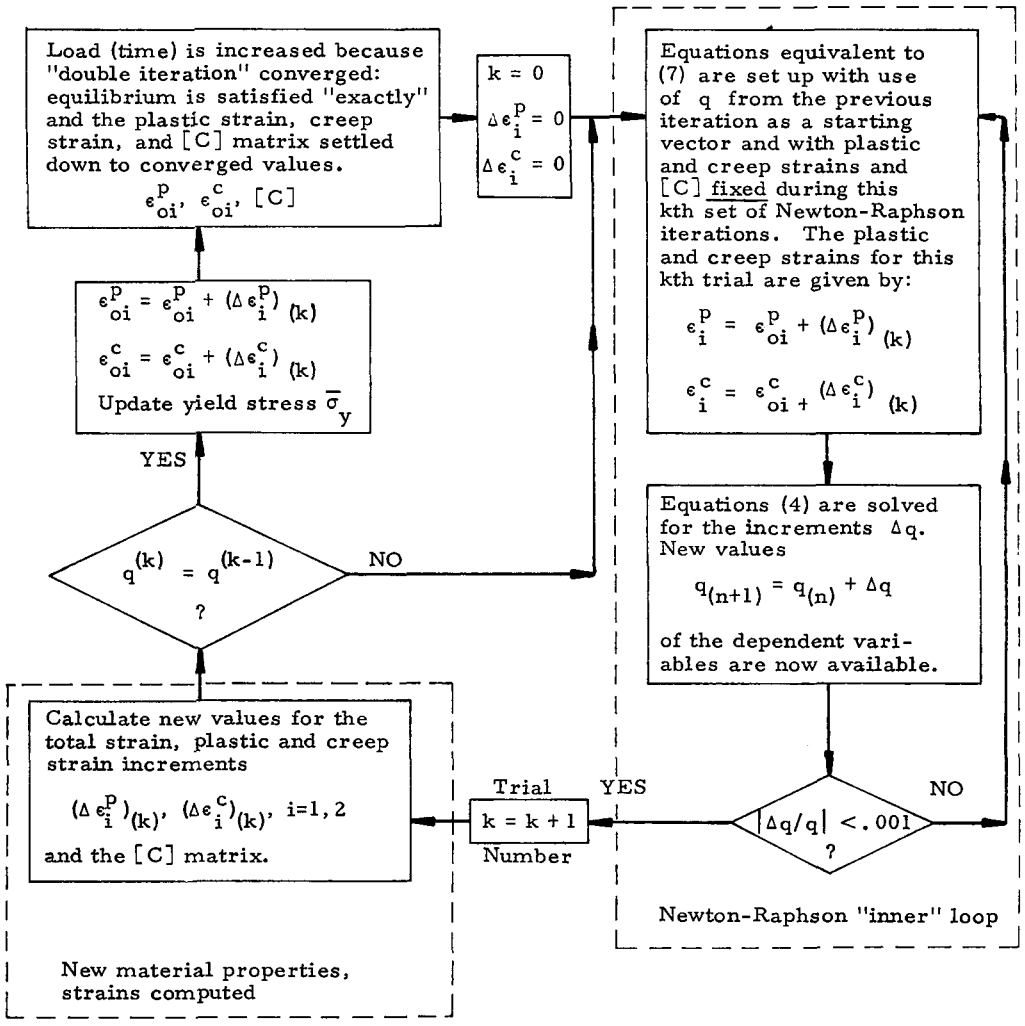

Figure 5. Flow chart of the double iteration loop used in BOSOR 5 for problems in which both material and geometrical nonlinearities exist

effective stress, $\bar{\sigma}_{(i-1)}$. In BOSOR 5 the criterion is

$$d\bar{\sigma}_{(i)}/\bar{\sigma}_{(i-1)} \leqslant 0{\cdot}01 \tag{25}$$

This strategy leads to subincrements of varying duration within the 'major' increment Δt.

Steps in the computational procedure

Suppose that the computer has just completed the calculations for a certain load state (0) and the load has just been increased. For the next load step the Newton–Raphson loop is entered without any change in the plastic or creep strains or $[C]$-matrix. This is the first trial, or $k = 0$ (see Figure 5). The Newton–Raphson iterations will presumably converge, and calculations of new plastic and creep strain increments will then begin with $k = k + 1 = 1$. The subsequent computational steps follow.

Step 1. Given the new displacement vector q, calculate the total strain components ε_1, ε_2.

Step 2. Assume that the elastic strain components are given by

$$\varepsilon_i^e = \varepsilon_i - \varepsilon_{0i}^p - \varepsilon_{0i}^c - \varepsilon_i^T \qquad (i = 1, 2) \tag{26}$$

Step 3. Calculate the stress components, effective stress

$$\sigma_1 = \frac{E}{1-\nu^2}(\varepsilon_1^e + \nu\varepsilon_2^e); \qquad \sigma_2 = \frac{E}{1-\nu^2}(\varepsilon_2^e + \nu\epsilon_1^e); \qquad \bar{\sigma} = (\sigma_1^2 + \sigma_2^2 - \sigma_1\sigma_2)^{1/2} \tag{27}$$

The quantity $\bar{\sigma}$ is shown in Figure 6.

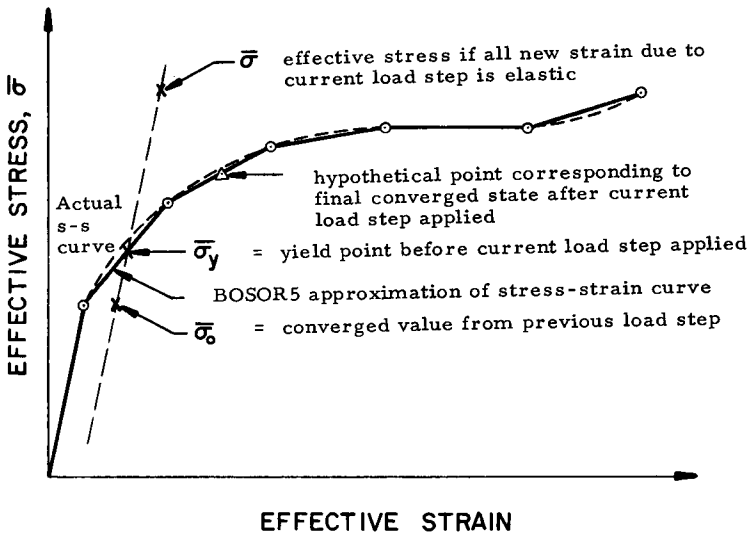

Figure 6. Actual stress–strain curve and BOSOR 5 model showing significant stresses used in the analysis

Step 4. If the effective stress is less than the yield stress $\bar{\sigma}_y$ (see Figure 6), compute the creep strain increment, set $[C] = 0$, and then go to Step *#11.*

Step 5. Calculate the elastic strain components corresponding to the last converged load step. Calculate the corresponding stress components and effective stress:

$$\sigma_{01} = \frac{E}{(1-\nu^2)}(\varepsilon_{10}^e + \nu\varepsilon_{20}^e), \quad \text{etc.} \qquad \bar{\sigma}_0 = f(\sigma_{10}, \sigma_{20}) \tag{28}$$

(see $\bar{\sigma}_0$ in Figure 5.)

Step 6. Is the effective stress on the yield surface at the beginning of the load step? If so, go to Step #8. If material creeps, go to Step #8 regardless of the position of $\bar{\sigma}_0$.

Step 7. If the effective stress is inside the yield surface at the beginning of the load step and if the material does not creep but does yield we must 'move out' to the yield surface before proceeding with the calculation of plastic strain increments. There exists a positive number μ between zero and unity such that

$$\sigma_{1y} = \sigma_{10} + \mu(\sigma_1 - \sigma_{10}); \qquad \sigma_{2y} = \sigma_{20} + \mu(\sigma_2 - \sigma_{20}) \tag{29}$$

In Eq. (29) σ_{1y}, σ_{2y} are the stress components corresponding to the point in Figure 5 labelled '$\bar{\sigma}_y$—yield point before current load step is applied'. The components σ_{10}, σ_{20} correspond to the point $\bar{\sigma}_0$, and σ_1, σ_2 correspond to the point $\bar{\sigma}$. The formula for μ is

$$\mu = \frac{1}{2(\overline{d\sigma})^2}\left[-b + \left[b^2 + 4(\overline{d\sigma})^2(\sigma_y^2 - \sigma_0^2)\right]^{1/2}\right] \tag{30}$$

where

$$\begin{aligned} b &\equiv d\sigma(2\sigma_{10} - \sigma_{20}) + d\sigma_2(2\sigma_{20} - \sigma_{10}) \\ d\sigma_1 &\equiv \sigma_1 - \sigma_{10} \qquad d\sigma_2 \equiv \sigma_2 - \sigma_{20} \\ (\overline{d\sigma})^2 &\equiv (d\sigma_1)^2 + (d\sigma_2)^2 - (d\sigma_1)(d\sigma_2) \end{aligned} \tag{31}$$

Step 8. The elastic strains corresponding to a state of stress on the yield surface are given by

$$\varepsilon^e_{1y} = \frac{1}{E}(\sigma_{1y} - \nu\sigma_{2y}); \qquad \varepsilon^e_{2y} = \frac{1}{E}(\sigma_{2y} - \nu\sigma_{1y}) \tag{32}$$

The elastic strains corresponding to the last converged load step are

$$\varepsilon^e_{10} = \frac{1}{E}(\sigma_{10} - \nu\sigma_{20}); \qquad \varepsilon^e_{20} = \frac{1}{E}(\sigma_{20} - \nu\sigma_{10}) \tag{33}$$

Define $\varepsilon^e_{ib} = \varepsilon^e_{iy}$ or ε^e_{i0}, where the 'b' signifies 'beginning elastic strain component'.

If the wall material is loaded into the plastic zone during the current load increment, the total strains ε_1, ε_2 are composed of the elastic strains at the beginning of the load step or elastic strains required to bring a point to the yield surface, plus the accumulated, known plastic and creep strains ε^p_{0i}, ε^c_{0i}, $(i = 1, 2)$ at the beginning of the load step, plus the thermal strains ε^T_i, plus the new elastic strains due to the current load step, $[(1/E)(\Delta\sigma_1 - \nu\,\Delta\sigma_2)$, etc.], plus the new plastic and creep strain increments, $\Delta\bar{\varepsilon}^p\{\partial\bar{\sigma}/\partial\sigma\}$ and $\Delta\bar{\varepsilon}^c\{\partial\bar{\sigma}/\partial\sigma\}$ due to the current load step.

The total strains are thus

$$\begin{aligned} \varepsilon_1 &= \varepsilon^e_{1b} + \varepsilon^p_{01} + \varepsilon^c_{01} + \varepsilon^T_1 + \frac{1}{E}(\Delta\sigma_1 - \nu\,\Delta\sigma_2) + (\Delta\bar{\varepsilon}^p + \Delta\bar{\varepsilon}^c)\frac{\partial\bar{\sigma}}{\partial\sigma_1} \\ \varepsilon_2 &= \varepsilon^e_{2b} + \varepsilon^p_{02} + \varepsilon^c_{02} + \varepsilon^T_2 + \frac{1}{E}(\Delta\sigma_2 - \nu\,\Delta\sigma_1) + (\Delta\bar{\varepsilon}^p + \Delta\bar{\varepsilon}^c)\frac{\partial\bar{\sigma}}{\partial\sigma_2} \end{aligned} \tag{34}$$

or, written in another way

$$\begin{aligned} \Delta\varepsilon_1 &= \frac{1}{E}(\Delta\sigma_1 - \nu\,\Delta\sigma_2) + (\Delta\bar{\varepsilon}^p + \Delta\bar{\varepsilon}^c)\frac{\partial\bar{\sigma}}{\partial\sigma_1} \\ \Delta\varepsilon_2 &= \frac{1}{E}(\Delta\sigma_2 - \nu\,\Delta\sigma_1) + (\Delta\bar{\varepsilon}^p + \Delta\bar{\varepsilon}^c)\frac{\partial\bar{\sigma}}{\partial\sigma_2} \end{aligned} \tag{35}$$

Equations (35) contain 3 unknowns: $\Delta\sigma_1$, $\Delta\sigma_2$, and $\Delta\bar{\varepsilon}^p$. ($\Delta\bar{\varepsilon}^c$ is a known function of $\bar{\sigma}$ and time, and $\bar{\sigma}$ is a known function of $\sigma_{iy} + \Delta\sigma_i$, in which σ_{iy} is known.) The third 'equation' needed for the solution is the given stress–strain curve in which an effective stress increment is related to an effective plastic strain increment. These simultaneous equations, called 'System B' in the Introduction, are non-linear and in fact are not entirely explicitly defined, since the

stress–strain curve is given as a sequence of straight lines and not as a continuous function. It is pointed out in the Introduction that unless a subincremental method is used these simultaneous non-linear equations may not have any solution.

Step 9. Establish the number of 'subincrements' to be used for evaluating the plastic and creep strain increments. If there is no creep:

$$\Delta\varepsilon_i = \varepsilon_i^{\mathrm{e}} - \varepsilon_{i\mathrm{b}}^{\mathrm{e}} \qquad (i = 1, 2)$$

$$\Delta\bar{\varepsilon} = \frac{2}{\sqrt{3}}(\Delta\varepsilon_1^2 + \Delta\varepsilon_2^2 + \Delta\varepsilon_1\,\Delta\varepsilon_2)^{1/2}; \qquad M = \Delta\bar{\varepsilon}/0{\cdot}0002 \quad (36)$$

M is the number of subincrements required at the current location in the shell wall, the current trial, and the current load step. If creep is present, establish the time subincrement such that the change in effective stress is less than one per cent of the current estimate of the effective stress. There is an additional requirement described in reference 5 that in cases of near-neutral loading the number of subincrements must be increased if the change in direction of the plastic strain increment vector is excessive during a subincrement. The number 0·0002 was chosen as a result of numerical experimentation.

Step 10. It is assumed that for each subincrement the subincremental resultant plastic strain is normal to the 'temporary' yield surface existing at the beginning of the subincrement

$$\mathrm{d}\varepsilon_i = \Delta\varepsilon_i/M \qquad (i = 1, 2) \quad (37)$$

For each subincrement the following equations must be solved:

$$\mathrm{d}\varepsilon_1 = \frac{1}{E}(\mathrm{d}\sigma_1^{(i)} - \nu\,\mathrm{d}\sigma_2^{(i)}) + (\mathrm{d}\bar{\varepsilon}_{(i)}^{\mathrm{p}} + \mathrm{d}\bar{\varepsilon}_{(i)}^{\mathrm{c}})B_1^{(i-1)} \quad (38)$$

$$\mathrm{d}\varepsilon_2 = \frac{1}{E}(\mathrm{d}\sigma_2^{(i)} - \nu\,\mathrm{d}\sigma_1^{(i)}) + (\mathrm{d}\bar{\varepsilon}_{(i)}^{\mathrm{p}} + \mathrm{d}\bar{\varepsilon}_{(i)}^{\mathrm{c}})B_2^{(i-1)}$$

in which

$$B_1^{(i-1)} = \frac{\partial\bar{\sigma}^{(i-1)}}{\partial\sigma_1^{(i-1)}} \qquad B_2^{(i-1)} = \frac{\partial\bar{\sigma}^{(i-1)}}{\partial\sigma_1^{(i-1)}} \quad (39)$$

where i refers to the ith subincrement.

The actual stress–strain curve is replaced with a sequence of straight line segments as shown in Figure 6. it is assumed that within any effective strain subincrement the stress–strain curve either has no corners or has only one corner. If a corner occurs within the subincrement, this subincrement is divided at the corner into two (in general unequal) subincrements. Hence, it always holds that within a subincrement

$$\mathrm{d}\bar{\varepsilon}_{(i)}^{\mathrm{p}} = \frac{E - E_{\mathrm{T}}}{EE_{\mathrm{T}}}[\bar{\sigma}^{(i)} - \bar{\sigma}^{(i-1)}] \quad (40)$$

where E_{T}, the local tangent modulus, is constant. Because of the small size of the subincrement, the expression $\bar{\sigma}_{(i)} - \bar{\sigma}_{(i-1)}$ can be linearized:

$$\bar{\sigma}^{(i)} - \bar{\sigma}^{(i-1)} = B_1^{(i-1)}\,\mathrm{d}\sigma_1^{(i)} + B_2^{(i-1)}\,\mathrm{d}\sigma_2^{(i)} \quad (41)$$

The creep law used in BOSOR 5 is of the form

$$\bar{\varepsilon}^{\mathrm{c}} = A\bar{\sigma}^m t_{\mathrm{e}}^n \quad (42)$$

in which t_e is derived as shown in Figure 7. The stress within a subincrement $dt^{(i)}$ is assumed to be constant and equal to the average of the stresses $(\bar{\sigma}_{i-1}+\bar{\sigma}_i)/2$ at the beginning and end of that subincrement. The effective creep strain accumulated during the subincrement $(\bar{\varepsilon}^c_i-\bar{\varepsilon}^c_{i-1})$ is calculated with the assumption that the material point follows the creep curve corresponding to the average stress starting at the effective time $t_e^{(i-1)}$ at the beginning of the subincrement (curve '2' in Figure 7). The new effective time $t_e^{(i)}$ at the end of the subincrement is determined from the new effective strain $\bar{\varepsilon}^c_i$, as shown in Figure 7.

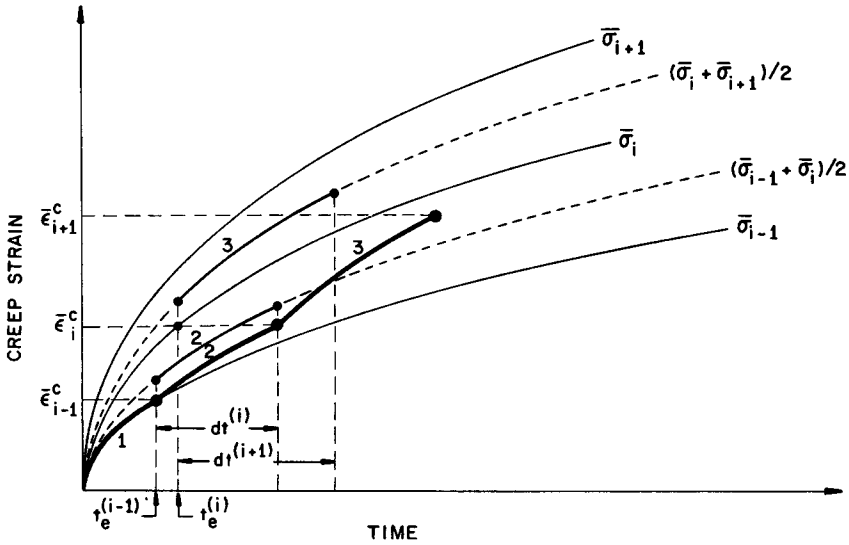

Figure 7. Creep strain accumulated during subincrements

This method is a sort of combination of the time hardening and strain hardening approaches. The time hardening element enters the picture because of the assumption that we are following the curve '2' in Figure 7 rather than a curve beginning at the earlier time at which the creep curve for $(\bar{\sigma}_{i-1}+\bar{\sigma}_i)/2$ yields the effective creep strain $\bar{\varepsilon}^c_{i-1}$. In most practical problems for which creep is significant most of the creep occurs at fairly constant stress levels. This situation is illustrated in Figure 8. The creep curve (a) is the same as that shown in Figure 4—derived from a strain hardening model corresponding to the stepped variation (a) in stress shown at the top of the figure. The creep curve (b) corresponds to the variation in stress indicated by the solid line (b) in the top frame. The strategy indicated in Figure 7 would yield lower creep strains than the strain hardening model only in the relatively brief intervals $t_1<t<t_2$ and $t_3<t<t_4$ when the stress level is being increased. Even this small effect would be somewhat counteracted by the fact that the effective times corresponding to the beginnings of the long intervals $t_2<t<t_3$ and $t_4<t<t_5$ would thus be earlier, leading to slightly greater creep strain increments accumulated during these long periods. From Eq. (42) and Figure 7 it can be seen that for each subincrement the effective creep strain subincrement is given by

$$d\bar{\varepsilon}^c_{(i)} = A\left(\frac{\bar{\sigma}_{(i)}+\bar{\sigma}_{(i-1)}}{2}\right)^m [(t_e^{(i-1)}+dt^{(i)})^n-(t_e^{(i-1)})^n] \tag{43}$$

in which the effective time at the beginning of the subincrement is

$$t_e^{(i-1)} = [\bar{\varepsilon}_{(i-1)}/A\bar{\sigma}^m_{(i-1)}]^{1/n} \tag{44}$$

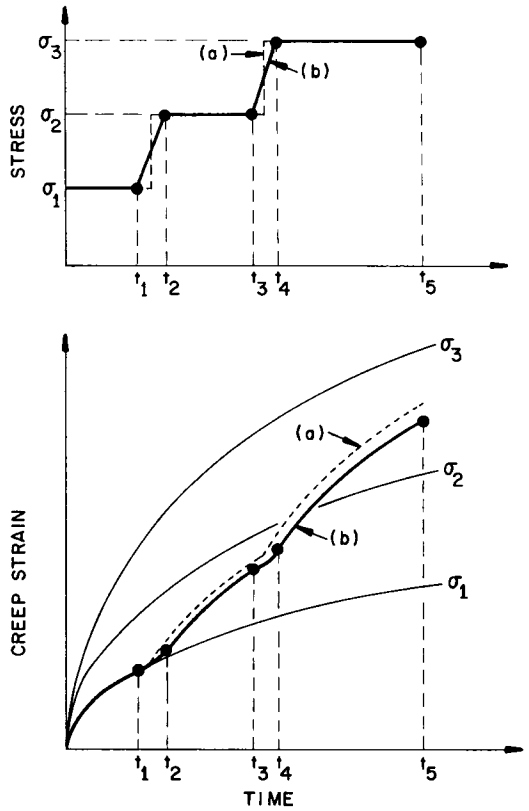

Figure 8. Accumulated creep strain for two similar loading programs

The effective creep strain subincrement can be expressed in terms of a known quantity plus a quantity dependent on the effective stress subincrement $d\bar{\sigma}_{(i)}$ through the expansion

$$\left(\frac{\bar{\sigma}_{(i)}+\bar{\sigma}_{(i-1)}}{2}\right)^m=\left(\bar{\sigma}_{(i-1)}+\frac{d\bar{\sigma}_{(i)}}{2}\right)^m=\bar{\sigma}_{(i-1)}^m\left(1+\frac{m\,d\bar{\sigma}_{(i)}}{2\bar{\sigma}_{(i-1)}}+\ldots\right) \tag{45}$$

The effective creep strain subincrement thus becomes

$$d\bar{\varepsilon}^{\,c}_{(i)}=A\bar{\sigma}_{(i-1)}^m[(t_e^{(i-1)}+dt^{(i)})^n-(t_e^{(i-1)})^n]\left(1+\frac{m\,d\bar{\sigma}_{(i)}}{2\bar{\sigma}_{(i-1)}}\right) \tag{46}$$

With the effective stress subincrement $d\bar{\sigma}_{(i)}$ given by

$$d\bar{\sigma}_{(i)}=B_1^{(i-1)}\,d\sigma_1^{(i)}+B_2^{(i-1)}\,d\sigma_2^{(i)} \tag{47}$$

and with use of Eqs. (40)–(46) in Eqs. (38), we obtain two equations for the unknowns $d\sigma_1^{(i)}$ and $d\sigma_2^{(i)}$, the subincremental stress components:

$$\begin{aligned}A_{11}\,d\sigma_1^{(i)}+A_{12}\,d\sigma_2^{(i)}&=d\varepsilon_1-A_0B_1^{(i-1)}\\A_{12}\,d\sigma_1^{(i)}+A_{22}\,d\sigma_2^{(i)}&=d\varepsilon_2-A_0B_2^{(i-1)}\end{aligned} \tag{48}$$

in which

$$A_{11}=\frac{1}{E}+\frac{1}{E^{**}}(B_1^{(i-1)})^2 \tag{49}$$

$$A_{12}=\frac{-\nu}{E}+\frac{1}{E^{**}}(B_1^{(i-1)})(B_2^{(i-1)})$$

$$A_{22}=\frac{1}{E}+\frac{1}{E^{**}}(B_2^{(i-1)})^2$$

$$\frac{1}{E^{**}}=\frac{1}{E^{*}}+\frac{A_0 m}{2\bar{\sigma}_{(i-1)}}$$

$$A_0=A\bar{\sigma}_{(i-1)}^{m}[(t_e^{(i-1)}+\mathrm{d}t^{(i)})^n-(t_e^{(i-1)})^n]$$

$$\frac{1}{E^{*}}=(E-E_T)/(EE_T) \quad \text{if stress is increasing}$$

$$\frac{1}{E^{*}}=0 \quad \text{if stress is decreasing}$$

$t_e^{(i-1)}$ given by Eq. (44).

It is assumed that the strain subincrements $\mathrm{d}\varepsilon_1$ and $\mathrm{d}\varepsilon_2$ are the known strain increments $\Delta\varepsilon_1$ and $\Delta\varepsilon_2$ times the ratio $\mathrm{d}t/\Delta t$, where $\mathrm{d}t$ is the time subincrement and Δt is the total 'major' time increment:

$$\begin{aligned} A_{11}\,\mathrm{d}\sigma_1^{(i)}+A_{12}\,\mathrm{d}\sigma_2^{(i)}&=\Delta\varepsilon_1\,\mathrm{d}t^{(i)}/\Delta t-A_0B_1^{(i-1)}\\ A_{12}\,\mathrm{d}\sigma_1^{(i)}+A_{22}\,\mathrm{d}\sigma_2^{(i)}&=\Delta\varepsilon_2\,\mathrm{d}t^{(i)}/\Delta t-A_0B_2^{(i-1)}\end{aligned} \tag{50}$$

From Eqs. (50) we must first determine the time subincrement $\mathrm{d}t^{(i)}$ such that the change in effective stress [Eq. (47)] is less than one per cent of the effective stress. This is done by iteration: A starting value of $\mathrm{d}t^{(i)}$ is

$$\mathrm{d}t_{\text{start}}=\Delta t(0{\cdot}0002/\Delta\bar{\varepsilon}) \tag{51}$$

where

$$\Delta\bar{\varepsilon}\equiv\frac{2}{\sqrt{3}}(\Delta\varepsilon_1^2+\Delta\varepsilon_2^2+\Delta\varepsilon_1\,\Delta\varepsilon_2)^{1/2} \tag{52}$$

Corresponding to this known value of $\mathrm{d}t^{(i)}$, the stress subincrements $\mathrm{d}\sigma_1^{(i)}$, $\mathrm{d}\sigma_2^{(i)}$ are determined from Eq. (50), and Eq. (47) is used to check whether or not the requirement $|\mathrm{d}\bar{\sigma}/\bar{\sigma}|\leqslant 0{\cdot}01$ is satisfied. If not, a smaller $\mathrm{d}t^{(i)}$ is chosen and $\mathrm{d}\sigma_1^{(i)}$, $\mathrm{d}\sigma_2^{(i)}$ are again calculated. This iterative process is continued until $|\mathrm{d}\bar{\sigma}/\bar{\sigma}|\leqslant 0{\cdot}01$. In Eq. (51), if $(0{\cdot}0002/\Delta\bar{\varepsilon})>1$, then $\mathrm{d}t_{\text{start}}=\Delta t$. A tally is kept of the time $\sum_{k=1}\mathrm{d}t^{(k)}$ accumulated during the increment Δt, and subincremental iterations are terminated when $\sum_{k=1}\mathrm{d}t^{(k)}=\Delta t$.

To summarize, the procedure under Step # 10 is to:

(a) Calculate $B_1^{(i-1)}$, $B_2^{(i-1)}$.

(b) Find E_T from the known value of $\bar{\varepsilon}_{(i-1)}^{p}+\bar{\sigma}^{(i-1)}/E$ and the piecewise linear stress–strain curve.

(c) Solve Eqs. (48) for $\mathrm{d}\sigma_1^{(i)}$, $\mathrm{d}\sigma_2^{(i)}$.

(d) Calculate the effective stress subincrement from Eq. (47), the effective plastic strain subincrement from Eq. (40), and the effective creep strain subincrement from Eq. (46).

(e) Add all increments to the base values to obtain the updated values $\sigma_1^{(i)}$, $\sigma_2^{(i)}$, etc.
(f) If a counter is less than M or if $\sum \mathrm{d}t < \Delta t$, go back to (a).

Step 11. With values established for stress components and plastic and creep strain components, the 2×2 matrix $[C]$ can now be calculated through the use of Eq. (24). The symmetric 2×2 tangent stiffness matrix $[D_T]$ (Eq. (15)) is then calculated. Everything is now determined for this particular thickness station, meridional point, load step, and trial.

Step 12. Carry out Steps 1–11 for the next thickness station at the same meridional point.

Step 13. If Steps 1–11 have been completed for all thickness stations in the current shell wall layer, perform the integrations indicated in Eqs. (5) and (14). The volume element is

$$\mathrm{d}V = r(1+z/R_1)(1+z/R_2)\,\mathrm{d}z\,\mathrm{d}s\,\mathrm{d}\theta \tag{53}$$

where r is the radius of a latitude through the reference surface, z is the normal outward distance from the reference surface to a material point, R_1 and R_2 are the meridional and normal circumferential radii of curvature, $\mathrm{d}s$ is the elemental meridional arc of reference surface, and $\mathrm{d}\theta$ is the elemental circumferential angle. The meridional and circumferential strains ε_i are expressed in terms of reference surface strains e_i and changes in curvature $\aleph_i$ by the following:

$$\varepsilon_i = (e_i - z\aleph_i)/(1+z/R_i); \qquad i = 1, 2 \tag{54}$$

With Eqs. (53) and (54) and the known thermal strain

$$\varepsilon^{\mathrm{T}} = \alpha_i\,\Delta T; \qquad i = 1, 2 \tag{55}$$

in which ΔT is the known temperature rise above the zero-stress condition, and with $[D_T]$, $[C]$, $\varepsilon_{0i}^{\mathrm{p}}$ and $\varepsilon_i^{\mathrm{c}}$ known at all thickness stations in the layer, the z-integrations of Eqs. (5) and (14) can be performed. Simpson's rule is used for this integration. Integration over s amounts to multiplication by the length of a finite difference element (see reference 6) and integration over θ amounts to multiplication by 2π.

Step 14. Perform above steps for all shell layers (different materials) at the current meridional station.

Step 15. Perform above steps for all meridional points in the current shell segment.

Step 16. Perform above steps for all shell segments.

EXAMPLES

Flat circular plate under concentrated load

Flat aluminium plates were tested by Levine *et al.*[18] This is a good configuration with which to verify the analysis and the strategy because both geometrical and material non-linearities are significant. Figure 9 shows the experimental and theoretical load-deflection curves. Levine *et al.* also performed an analysis and also obtained good agreement with the test results. They used about 100 load steps, however.

Figure 3, discussed in the Introduction, shows the paths in stress and strain space followed by a material point as the load is increased from 0 to 1,000 lb. The final prediction of the state of stress and strain at $P = 1{,}000$ lb converges rapidly with increasing number of load steps. This rapid convergence can be attributed to the fact that at every load level utmost care has been

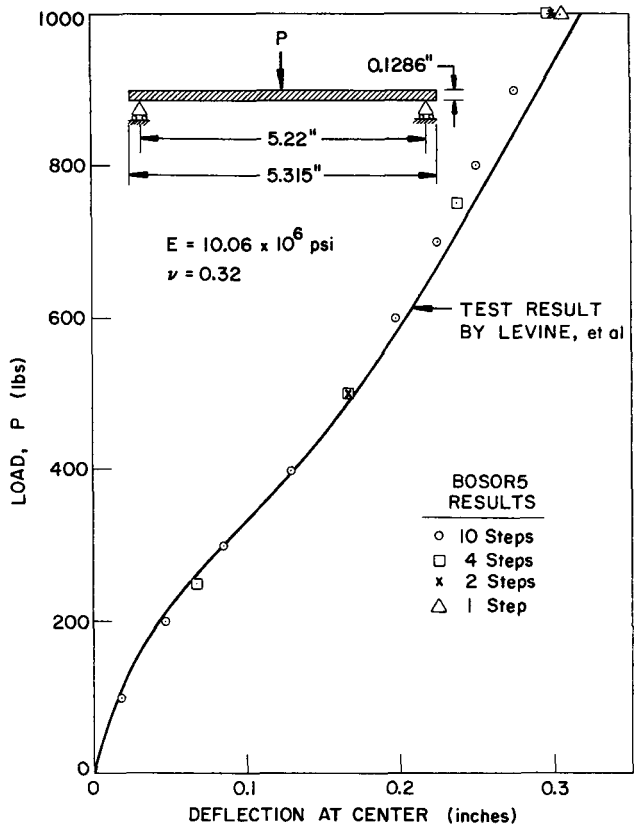

Figure 9. Load-deflection curves from test and BOSOR 5 for centrally loaded flat circular plate

taken, through Newton–Raphson iterations and the subincremental process, to assure convergence with respect to both geometrical and material non-linear behaviour.

Figure 10 shows the convergence of the displacement with 'trial' number. (A 'trial' is defined in Figure 5. One 'trial' represents a solution of the non-linear equation System A.) In this case a very large load increment, $\Delta P = 500$ lb, is used. Even so, the converged displacement is very close to the experimental result, as seen from the location of the 'X' corresponding to $P = 500$ lb in Figure 9. Nine trials were required in order to achieve convergence of the displacement distribution within a tolerance of 0·1 per cent. The first Newton–Raphson iteration on the first trial yields the linear elastic solution. This BOSOR 5 solution ($w_{max} = 0{\cdot}08718$ in) agrees with the formula tabulated in Roark[19] ($w_{max} = 0{\cdot}08703$ in). Throughout the first trial the material is treated as elastic, since this is the first load step and thus no previous history of plastic flow exists. Four Newton–Raphson iterations are required in this first trial for convergence to the non-linear elastic solution. The solution vector thus obtained is used as input for the determination of how much plastic flow occurs, and a new solution is obtained after five Newton–Raphson iterations in Trial #2. Two Newton–Raphson iterations are required for convergence in each of trials four–eight, and a ninth trial is required to ensure that the change in material properties between Trial #8 and Trial #9 is so slight that it affects the displacement vector by less than 0·01 per cent. The predicted maximum normal displacement is 0·17532 in.

Figure 11 demonstrates the subincremental method. This figure applies to one particular point in the circular plate. The point is located on the upper surface at a distance 0·4374 in from

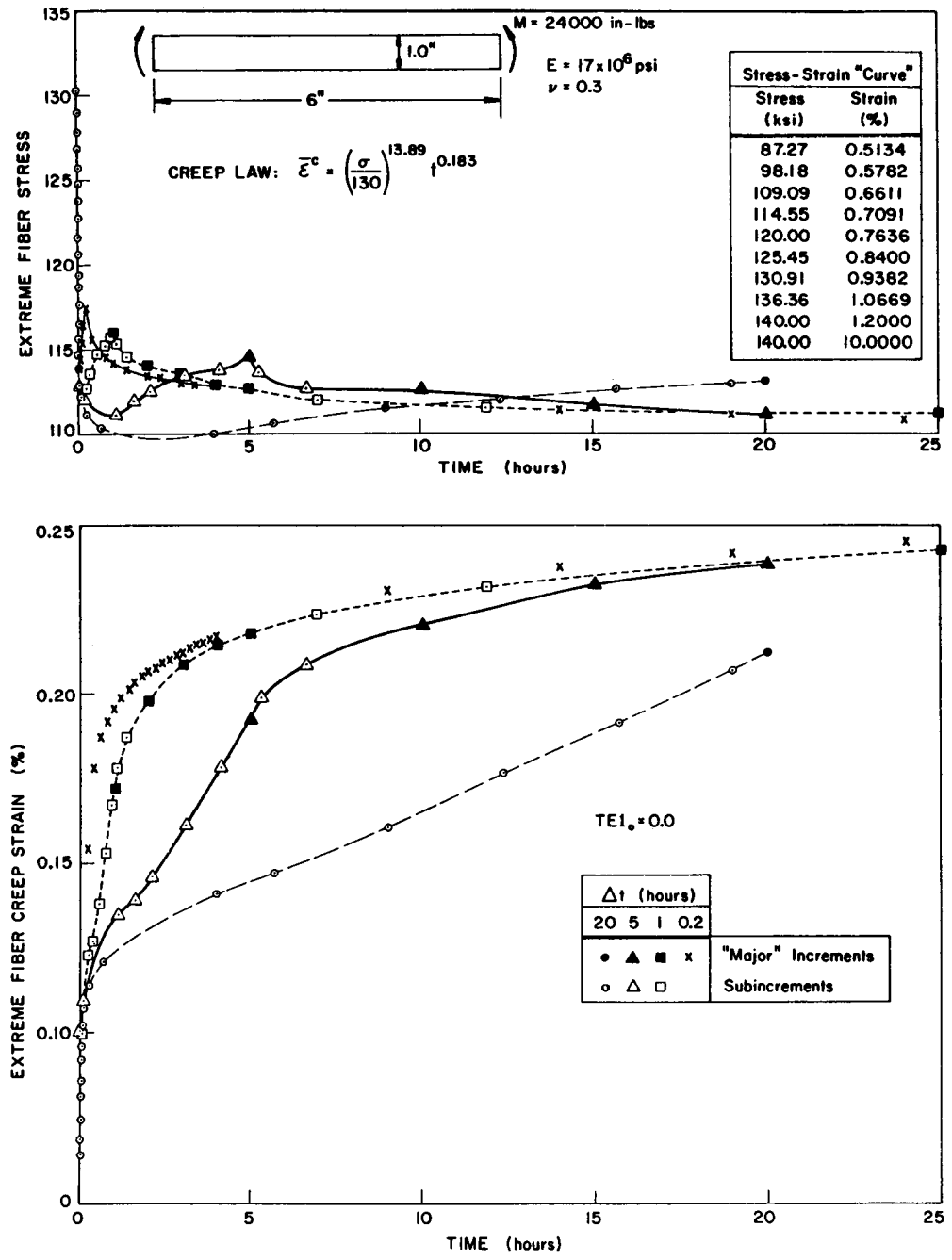

Figure 13. Extreme fibre stress and creep strain in the titanium beam as functions of time predicted with use of various time increments

is applied at time $t = 0$ and held constant. Thus, as time increases, the stress near the extreme fibres of the beam relaxes and the stress near the neutral axis increases such that equilibrium is maintained. Note that most of the change in stress from the instantaneous elastic-plastic distribution occurs within the first 0·2 h after application of the load. This phenomenon raises

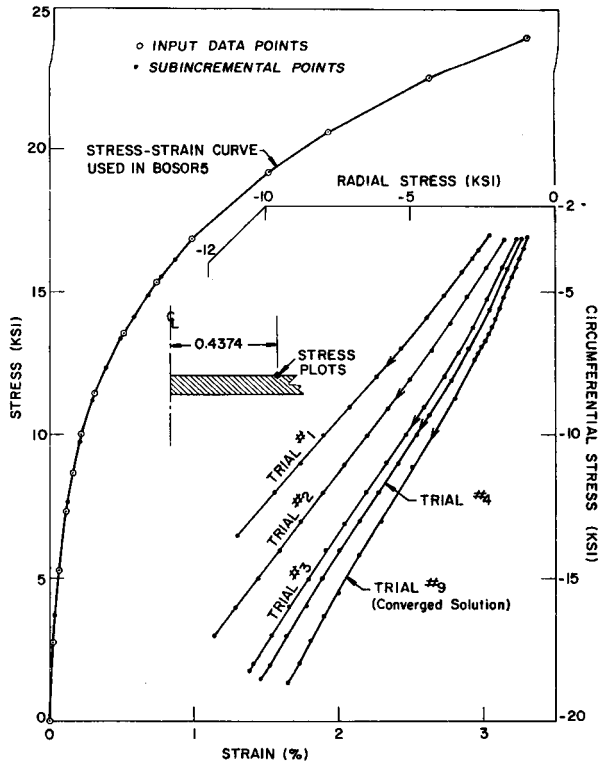

Figure 11. Paths in stress space followed by a material point in the plate during the subincremental process for successive trials

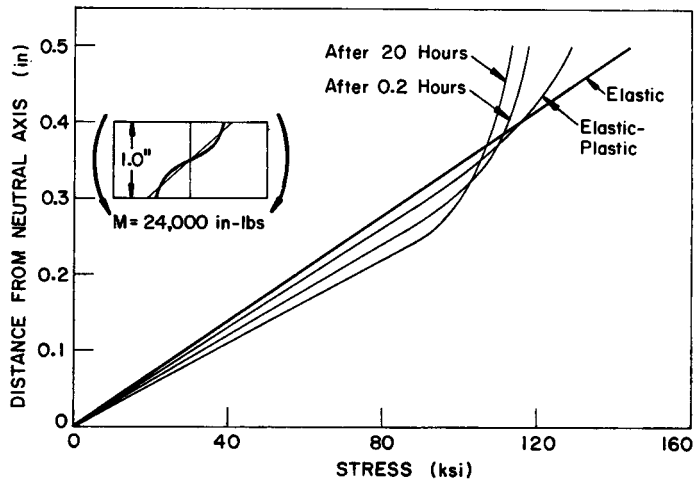

Figure 12. Stress distribution in a titanium beam under constant bending moment

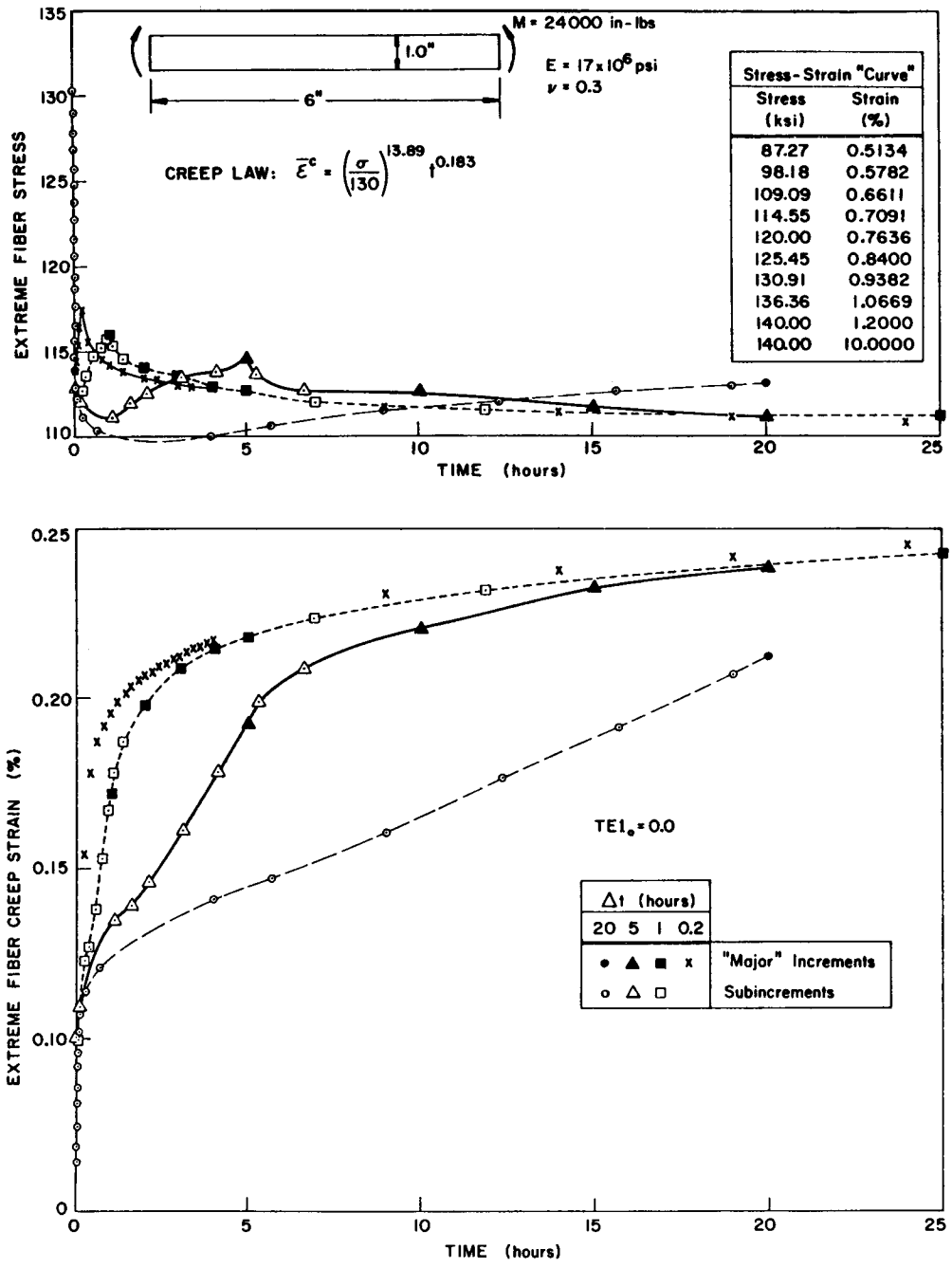

Figure 13. Extreme fibre stress and creep strain in the titanium beam as functions of time predicted with use of various time increments

is applied at time $t = 0$ and held constant. Thus, as time increases, the stress near the extreme fibres of the beam relaxes and the stress near the neutral axis increases such that equilibrium is maintained. Note that most of the change in stress from the instantaneous elastic-plastic distribution occurs within the first 0·2 h after application of the load. This phenomenon raises

the question of just how much of the early time creep should be regarded as instantaneous plastic flow, a question that will not be dealt with here. The purpose of this example is to illustrate the subincremental strategy and the effect of changes of the major time increment on the predicted creep strain and extreme fibre stress.

Figure 13 shows the predicted extreme fibre stress and creep strain as functions of time for various time increments Δt. For $\Delta t = 1{\cdot}0$, $5{\cdot}0$, and $20{\cdot}0$ h, the values for each subincrement dt are also plotted. For $\Delta t = 0{\cdot}2$ h, subincremental values are shown only in the top frame and only for time less than $0{\cdot}2$ h. In two of the cases, those labelled $\Delta t = 0{\cdot}2$ and $\Delta t = 1{\cdot}0$, the time increment is increased after about 5 h of elapsed time.

Notice that in order that the criterion $|\Delta\bar{\sigma}/\bar{\sigma}| < 0{\cdot}01$ be satisfied many subincrements are required for very early times and fewer for later times. This is particularly evident in the curves corresponding to Δt equal to 20 h. Also, notice that during the first time increment the subincremental process leads to an erroneous prediction that the stress decreases from about 130 ksi initially to a minimum value that depends on Δt and then increases somewhat. The reason for this 'undershoot' is not known.

If the stresses predicted with use of the smallest time increment $\Delta t = 0{\cdot}2$ are regarded as the converged values, it is seen that use of $\Delta t = 1{\cdot}0$, $5{\cdot}0$, and $20{\cdot}0$ leads to overestimation of the stress at time $= 1{\cdot}0$, $5{\cdot}0$, $20{\cdot}0$ h, respectively. The too high stress leads to overestimation of the creep rate during the ensuring time increment. This trend continues to a diminishing degree in successive time increments until the predicted stresses and creep strains for all major time increments are reasonably close to one another. Thus, the error incurred in the early time increments due to the use of a large time increment is 'washed out' as time progresses. The results in Figure 13 indicate that if the analyst wants to know the state of stress and strain at time t, he should use a time increment of about $t/5$. For example, the results at $t = 20$ h are accurately predicted with use of $\Delta t = 5$ h; the results at $t = 5$ h are accurately predicted with use of $\Delta t = 1{\cdot}0$ h.

CONCLUSIONS

The principal advantages of the subincremental technique are the increased reliability with which problems involving non-linear plastic and time-dependent material behaviour can be solved and the greatly relaxed requirement on the number of load or time increments needed for satisfactory results. The advantage of the double iteration loop at each load level or time, that is, the removal of the calculation of tangent stiffness from the Newton–Raphson iterations, is that the numerical instability associated with erroneous prediction of alternative loading and unloading disappears.

The strategy described here is particulary well suited to the solution of problems involving discretization of one independent spacial variable, since such cases are associated with stiffness matrices with small bandwidths. Thus, the time required to perform the Newton–Raphson iterations at each trial and at each load level or time step is not excessive. One can afford to impose rigorous conditions on convergence. For problems involving discretization in two or three dimensions, some modifications of the strategy would be beneficial. It should be possible to vary the convergence criteria dynamically such that less computer time is spent during early trials at a given load level than during later trials. For example, one would not need cenvergence of the Newton–Raphson iterations to within $0{\cdot}1$ per cent in the first trial if subsequent changes in the tangent stiffness matrix were to affect the deformation at that load level or time step by many times that amount. A similar argument holds for the number of subincrements used for the determination of the plastic and creep strain increments. Fewer subincrements would suffice for earlier trials. The maximum number of trials allowed at each load level or time could also be

programmed in advance to vary during a case. Allowing for these and other modifications of a similar nature, it should be possible to apply the strategy described here to other more general problems.

ACKNOWLEDGEMENTS

This research was sponsored partly by the Lockheed Missiles and Space Company's Independent Research and Independent Development Programs. The development of the BOSOR 5 computer code was sponsored by the Naval Ship Research and Development Center, Carderock, Maryland, under Contract N00014–73–C–0065. Dr. Rembert Jones and Miss Joan Roderick were the technical monitors.

APPENDIX

Nomenclature

B	See Eq. (39)
$[C]$	2×2 matrix given by Eq. (24)
$[D]$	2×2 matrix: $[D]=\frac{E}{1-\nu^2}\begin{bmatrix}1 & \nu\\ \nu & 1\end{bmatrix}$
$[D_T]$	Tangent stiffness matrix, Eq. (15)
ε	Strain anywhere in the shell wall
E	Young's modulus
E_T	Tangent modulus
M	Number of subincrements within an increment
N	Number of degrees-of-freedom in problem
q_i	ith nodal point degree-of-freedom
t	Real time
t_e	Effective time, Eq. (44)
Δt	Time increment
dt	Time subincrement
T	Temperature
U	Strain energy
V	Volume
W	Work done by external forces
ν	Poisson's ratio
Ψ_i	Gradient of energy with respect to q_i
σ	Stress

Subscripts

1, 2	Meridional, circumferential directions
(i)	ith subincrement
0	Converged value at previous time or load
y	Yield
b	Value at the beginning of the subincremental process

Superscripts

c	Creep
e	Elastic
p	Plastic
T	Thermal or transpose, depending on context
$\bar{(\ )}$	'Effective' (e.g., $\bar{\sigma}$ = effective stress)
(i)	ith subincrement
m	Power on stress in the creep law
n	Power on time in the creep law

Symbols

$\lfloor\ \rfloor$	Row vector
$\{\ \}$	Column vector
$[\ ]$	Matrix
$\Delta(\ )$	Increment
$d(\ )$	Subincrement

REFERENCES

1. J. R. Tillerson, J. A. Stricklin and W. E. Haisler, 'Numerical methods for the solution of nonlinear problems in structural analysis', in *Numerical Solution of Nonlinear Structural Problems*, (ed. R. Hartung), AMD Vol. 6, *ASME*, New York, 1973, pp. 67–101.
2. H. Armen, 'Plastic analysis', in *Structural Mechanics Computer Programs*, (ed. W. Pilkey, K. Saczalski and H. Schaeffer), University press of Virginia, Charlottesville, 1974, pp. 37–79.
3. R. E. Nickell, 'Thermal stress and creep', in *Structural Mechanics Computer Programs*, (Ed. W. Pilkey, K. Saczalski and H. Schaeffer), University Press of Virginia, Charlottesville, 1974, pp. 103–122.
4. B. Hunsaker, Jr., D. K. Vaughan and J. A. Stricklin, 'A comparison of the capability of four hardening rules to predict a materials plastic behaviour', *2nd Nat. Cong. Pressure Vessels and Piping, ASME* Paper 75-PVP-43 (1975).
5. D. Bushnell, 'Large deflection elastic-plastic creep analysis of axisymmetric shells', *Numerical Solution of Nonlinear Structural Problems*. (Ed. R. F. Hartung), AMD Vol. 6, *ASME*, 1973, pp. 103–138.
6. D. Bushnell, 'BOSOR 5—Program for buckling of elastic-plastic complex shells of revolution including large deflections and creep', to appear, *Computers & Structures* (1976).
7. N. G. Huffington, 'Numerical analysis of elastoplastic stresses', Memorandum Report No. 2006, Ballistic Research Laboratories, Aberdeen Proving Ground, Maryland (1969).
8. G. C. Nayak and O. C. Zienkiewicz, 'Elastic-plastic stress analysis. A generalization for various constitutive relations including strain softening', *Int. J. num. Meth. Engng*, **5**, 113–135 (1972).
9. J. A. Stricklin, W. E. Haisler and W. A. von Riessemann, 'Formulation, computation, and solution procedures for material and/or geometric nonlinear structural analysis by the finite element method', SC-CR-72 3102, Sandia Laboratories, Albuquerque, New Mexico (1972).
10. W. L. Greenstreet, J. M. Corum, C. E. Pugh and K. C. Liu, 'Currently recommended constitutive equations for inelastic design analysis of FFTF components', (ORNL-TM-3602), Oak Ridge National Laboratory (1971).
11. Y. N. Rabotnov, 'Some problems on the theory of creep', Vestnik Moskovskovo University, **10**, 81 (1948), English Translation by S. Reiss, N.A.C.A. TM 1353 (1953).
12. Y. R. Rashid, 'Part I, Theory report for CREEP-PLAST computer program: Analysis of two-dimensional problems under simultaneous creep and plasticity', GEAP-10546, AEC R & D Report (1972); 'Part II: User's manual for CREEP-PLAST computer program', GEAP-13262-1, AEC R & D Report (1972).
13. A. D. Russel and A. S. Kobayashi, 'Short-time creep response of 6% Al-4% V titanium alloy subjected to variable uniaxial tensile loading', *Joint International Conference on Creep, Inst. Mech. Engineers*, London (1963).
14. P. Sharifi and D. N. Yates, 'Nonlinear thermo-elastic-plastic and creep analysis by the finite element method', *AIAA* Paper 73-358, *AIAA/ASME/SAE 14th Structures, Structural Dynamics, and Materials Conf.*, Williamsburg, Va. (1973). *AIAA J.*, **12**, 1210–1215 (1974).
15. O. C. Zienkiewicz and I. C. Cormeau, 'Viscoplasticity-plasticity and creep in elastic solids—a unified numerical approach', *Int. J. num. Meth. Engng*, **8**, 821–845 (1974).
16. C. Crussard, 'Transient creep of materials', *Joint Int. Conf. on Creep, Inst. Mech. Engrs*, London, 123–128 (1963).

17. P. V. Marcal, 'Finite-element analysis with material nonlinearities—theory and practice', in *Recent Advances in matrix Methods of Structural Analysis and Design*, University of Albama Press, 1971, pp. 257–282.
18. H. S. Levine, H. Armen, Jr., R. Winter and A. Pifko, 'Nonlinear behaviour of shells of revolution under cyclic loading', Grumman Research Department Report RE–426J (1972), Grumman Aerospace Corporation, Bethpage, New York. Also *Nat. Symp. on Computerized Structural Analysis and Design*, Washington, D.C. (1972).
19. R. J. Roark, *Formulas for stress and strain*, 3rd ed., Chap. 10, Art. 55, Case #2, 194, McGraw-Hill, New York, 1954.
20. H. P. Chu, 'Room temperature creep and stress relaxation of a titanium alloy', *J. Materials*, **5**, 633–642 (1970).